Chemistry

Physical & Theoretical Chemistry fields

Okayama University *Year* 2003

Role of additives for copper damascene electrodeposition experimental study on inhibition and acceleration effects

Kazuo Kondo
Okayama University

Toshiaki Matsumoto
Okayama University

Keiji Watanabe
Okayama University

This paper is posted at eScholarship@OUDIR : Okayama University Digital Information Repository.

http://escholarship.lib.okayama-u.ac.jp/physical_and_theoretical_chemistry/15

Journal of The Electrochemical Society, **151** (4) C250-C255 (2004)
0013-4651/2004/151(4)/C250/6/$7.00 © The Electrochemical Society, Inc.

Role of Additives for Copper Damascene Electrodeposition

Experimental Study on Inhibition and Acceleration Effects

Kazuo Kondo,*,z Toshiaki Matsumoto, and Keiji Watanabe*

Department of Applied Chemistry, Okayama University, Okayama 700-0082, Japan

The role of copper Damascene additives is discussed based on electrodeposit morphology on a through-mask cathode, field emission-Auger (FE-Auger), quartz crystal microbalance (QCM), and electrochemical measurements. Adsorbed particles, several tens of nanometers in diameter were observed on copper-electrodeposited surfaces by field emission-scanning electron microscopy (FE-SEM). These particles show a stronger oxygen intensity peak by FE-Auger spectrum than bare electrodeposited surfaces. The QCM frequency deviation did not increase with time in the $CuSO_4$ and H_2SO_4 bath without polyethylene glycol (PEG) and chloride ion (Cl^-) additives. When the substrates were immersed in the bath with these additives, the deviation markedly increased with time. Numerous PEG molecules were observed by FE-SEM immersed after 1000 s. The current density remained constant at a low value for the bath with PEG and Cl^- additives. The current density started to increase markedly with time just after adding 1 ppm of bis(3-sulfopropyl) disulfide (SPS). Numerous PEG molecules were present on the electrodeposits before adding SPS. No PEG molecules, however, remained on the surface once SPS was added to the bath. The current density increased with narrower opening widths of the through-mask cathode. Despite this increase, the deposit cross sections on narrower opening widths of 2 and 10 μm were flat and no curvatures were found. Hence, the deposit curvature is not the origin of the acceleration effect.
© 2004 The Electrochemical Society. [DOI: 10.1149/1.1649235] All rights reserved.

Manuscript submitted June 19, 2003; revised manuscript received November 4, 2003. Available electronically February 23, 2004.

Recently on-chip metallization has shifted from an aluminum to a copper process. In the copper Damascene process, the copper is electrodeposited into submicrometer blind vias and trenches. Recently, larger size vias of several tens of micrometers have been widely used to build up printed circuit boards (PCB) because vias can be stacked. Successful via filling requires the use of a combination of additives, *e.g.*, polyethylene glycol (PEG), chloride ions (Cl^-), bis(3-sulfopropyl) disulfide (SPS), and Janus green B (JGB). PEG and Cl^- additives produce an inhibitory effect while SPS produces an acceleratory effect.

Yokoi *et al.*[1] investigated the inhibitory effects of PEG and Cl^- with current-density/potential curves. They proposed a model that cuprous ions were held by PEG molecules and that these PEG molecules could be adsorbed on the copper surface in the presence of Cl^- ion. Kelly and West[2,3] used a quartz crystal microbalance (QCM) and electrochemical impedance spectroscopy (EIS) and found that PEG inhibits the copper electrodeposition reaction in the presence of Cl^-. Kelly *et al.*[4] further measured the current-density/potential curves for PEG, Cl^-, SPS, and JGB. Andricacos *et al.*[5] calculated the current density distribution of Damascene electrodeposition based on an inhibiting additive model of diffusion control. The inhibiting additive adsorbs preferentially on the outside of blind vias and trenches and inhibits electrodeposition. Kondo *et al.*[6] recently interpreted the current density distribution during via filling in terms of regions in the current-density/potential curves. Adsorbed PEG molecules about 30 nm in diameter were observed by field-emission scanning electron microscopy (FE-SEM) for the first time by Kondo *et al.*[7-9] These molecules preferentially absorb at the edges of macrosteps and inhibit the lateral growth of the copper electrodeposit. With JGB, these molecules become diffusion controlled and adsorb preferentially on the outside of blind vias and trenches.

Reid[10] suggested initially that the acceleration effect is related to SPS adsorption on the electrodeposit surface. Josell *et al.*[11] and West *et al.*[12] independently proposed mathematical models based on SPS adsorption. As the copper Damascene electrodeposition proceeds, the bottom area shrinks and increases in curvature. The adsorbed SPS accumulates on this curvature and accelerates the bottom-up filling.

Deligianni *et al.*[13] suggested that the acceleration effect is caused by the catalytic effect of the copper ion and SPS complex, and this complex accumulates inside the vias of smaller features. Farndon[14] proposed the existence of cuprous and thiolate complex. Recently, Kondo *et al.*[7-9] monitored the via bottom acceleration effect by using a through-mask cathode and suggested that the cuprous and thiolate complex accelerates the deposition effect at the via bottom. It was found that current densities increased with increasing the via depth. The deeper the via is, the larger the current density. With a conventional flat-plate cathode, the current-density/potential curves of $Cl^- + PEG + SPS$, $Cl^- + PEG + JGB$, and $Cl^- + PEG + JGB + SPS$ are almost identical. With a through-mask cathode, the current densities increase markedly with SPS. Moreover, Vereecken *et al.*[15] detected the free acceleration complex on the ring of rotating glassy carbon—platinum disk electrode.

The objective of this paper is to report detailed experimental results on Damascene electrodeposition additives of Cl^-, PEG, and SPS. The inhibitory effect was observed by FE-SEM, field emission Auger (FE-Auger), and QCM. The acceleration effect was analyzed by deposition on a through-mask cathode, examination of deposit cross sections, and deposition on a glassy carbon ring-disk electrode.

Experimental

Table I shows the bath composition. The basic bath consists of $CuSO_4$ and H_2SO_4 of 0.6×10^3 and 1.85×10^3 mol/m^3, respectively. Additives are Cl^-, PEG of 7500 molecular weight, and JGB, whose concentrations are shown in Table I. The bath was used for

Table I. Bath composition.

Basic bath	
$CuSO_4 \cdot 5H_2O$	0.60 mol/L
H_2SO_4	1.85 mol/L
Additives	
PEG (Polyethylene glycol)	400 mg/L
HCl	100 mg/L
JGB (Janus Green B)	10 mg/L
SPS (Bis(3-sulfopropyl) disulfide)	1 mg/L

* Electrochemical Society Active Member.
z E-mail: kkondo@cc.okayama-u.ac.jp

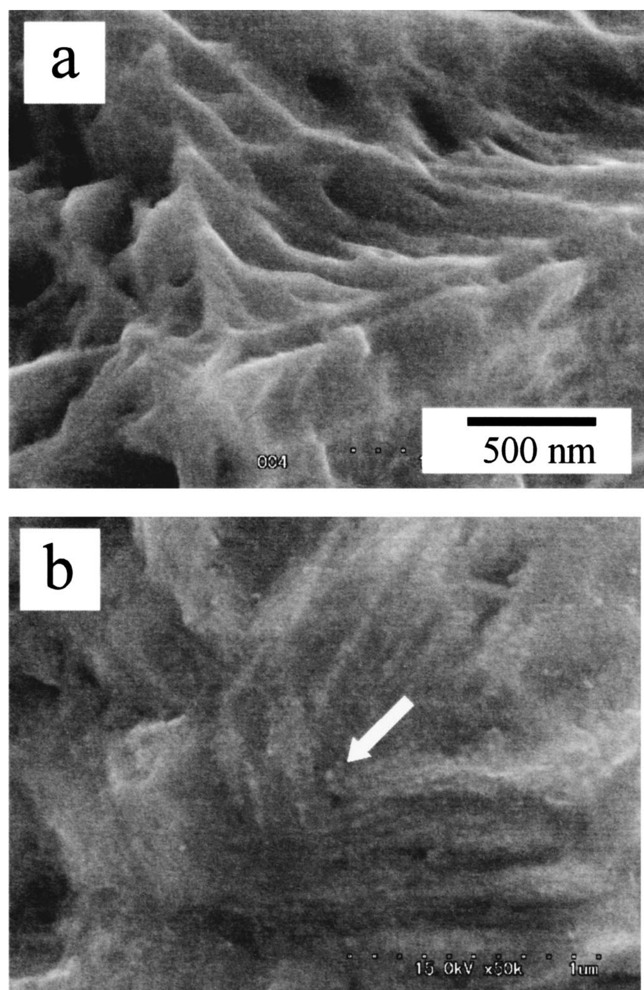

Figure 1. FE-SEM micrograph of electrodeposits with PEG and Cl^- additives. (a) Electrodeposition time of 15 and (b) 60 min.

each experiment 1 h after bath preparation. The potential was kept constant of −200 mV from the rest potential *vs.* 3.33 mol/L KCl-AgCl, unless otherwise specified.

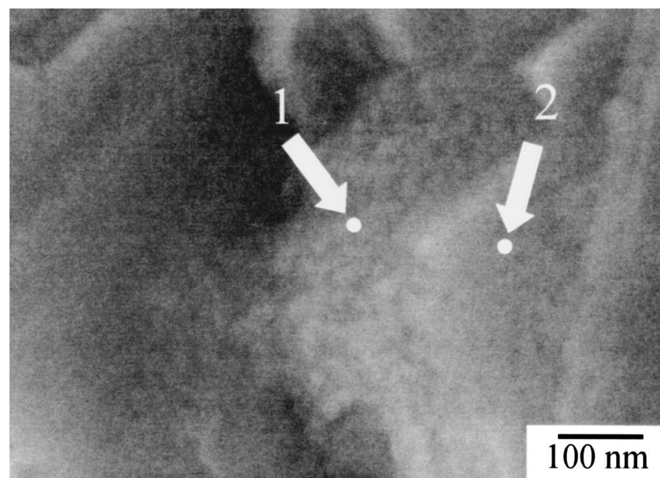

Figure 2. FE-SEM micrograph of electrodeposits with PEG and Cl^- additives. Point 1, with adsorbed particles and point 2, without particles.

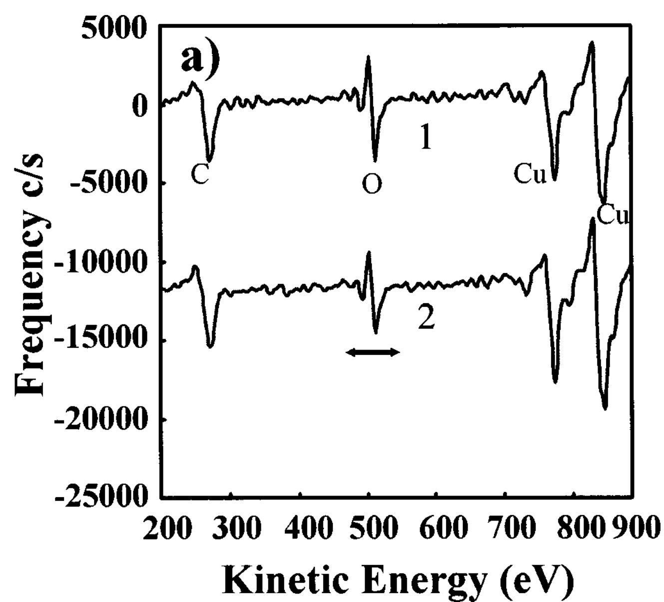

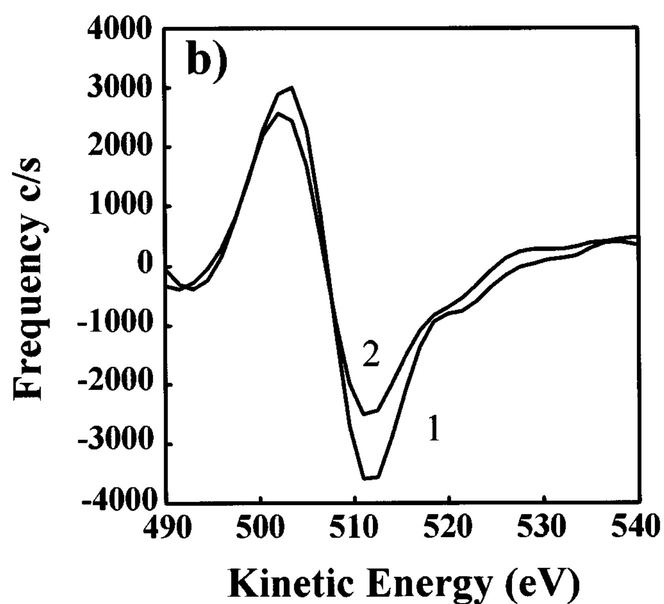

Figure 3. FE-Auger spectra of points 1 and 2 in Fig. 2. (a) Auger spectra at point 1 and 2; and (b) Auger spectra of enlarged oxygen peak.

The morphology of electrodeposits was observed by FE-SEM (Hitachi S-4300). FE-Auger (Smart-200, Physical Electronics) was used to measure the Auger spectrum of oxygen, carbon, and copper at the local points of the electrodeposits. The space resolution of this FE-Auger was about 10 nm.

A QCM (HQ-series, Hokuto-denko) was connected to the potentiostat of a HZ-3000 (Hokuto-denko). A 6 MHz quartz gold electrode substrates were initially electrodeposited with pure copper from a basic bath consisting only of only $CuSO_4$ and H_2SO_4. The substrates were immersed in the additive-containing electrolyte and frequency deviation-time curves were measured. The current density-time curves were measured with a rotating disk electrode (RDE) 12 mm in diameter.

The through-mask cathodes were prepared as follows. Photoresist patterns were formed on copper foil. The patterns consisted of 30 μm wide lines of exposed copper foil surface with widths of 2, 10, and 30 μm. The pattern had ten lines of 16 mm length and 1.0 mm pitch. THB-430N (JSR Co.) photoresist was used. The photo-

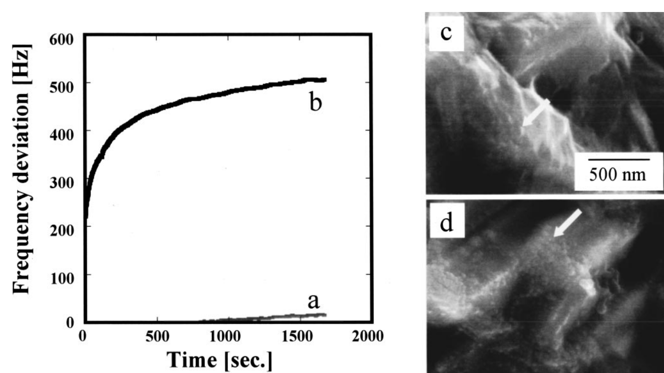

Figure 4. QCM measurements on Cu electrodeposited surface. (curve a) Frequency deviation-time curves without PEG and Cl^- additives; (curve b) with PEG and Cl^- additives. (c) FE-SEM micrograph of electrodeposits immersed into the electrolyte with PEG and Cl^- additives for 200 s and (d) for 1000 s.

resist patterns were then attached to the RDE. The cathodes were then subjected to potentiodynamic polarization from 100 to -400 mV (*vs.* Ag/AgCl sat. KCl). In addition, cathodic polarization in the bath with PEG, Cl^-, and SPS additives was performed in an RDE to detect the existence of an free-accelerant complex. The rotating ring-disk electrode consisted of a glassy-carbon ring and glassy-carbon disk. The bath was the same as that used in current-density curve measurements for the through-mask cathode except that the SPS concentration was 80 ppm to improve detection.

The encapsulated specimens, prepared by imbedding them in epoxy resin, which was cut perpendicular to the copper surface and polishing. They were examined under a scanning electron microscope (SEM).

Results

Inhibition effect.—Figure 1 shows a FE-SEM micrograph of electrodeposits with PEG and Cl^- additives. Figure 1a shows electrodeposits after 15 min and (b) after 60 min of deposition. In Fig. 1a the electrodeposits had crystal diameters of 500 μm with flat surfaces. Note several 10 nm particles are present. However in Fig. 1b, the crystal surface is not flat, and several 10 nm particles are observed (see arrow in Fig. 1b). The crystal diameter is 500 μm. Adsorption of these several 10 nm particles on the electrodeposited copper surface depends on the electrodeposition time.

Identification of the particles by FE-Auger spectroscopy.—Figure 2 is a FE-SEM micrograph of an electrodeposit formed in the presence of PEG and Cl^- additives after 120 min electrodeposition time. At the center of the micrograph, several 10 nm particles are densely adsorbed. The white arrow labeled 1 indicates the densely adsorbed particles, and the white arrow labeled 2 indicates an area without particles.

Figure 3 is a FE-Auger spectrum corresponding to the points indicated by arrows 1 and 2 in Fig. 2. In Fig. 3a, a carbon peak exists at 295 eV, an oxygen peak at 517 eV and copper peaks at 795 and 860 eV. Carbon and copper have almost the same peak intensity. Oxygen at point 1, however, has a stronger peak intensity than point 2. Figure 3b is an enlarged spectrum from 490 to 540 eV. At 517 and 503 eV, the oxygen peak intensity is stronger for point 1 where several 10 nm particles are densely adsorbed.

PEG is $(C_2H_5O_2)_n$ and the atomic number of oxygen is same as carbon. The densely adsorbed several 10 nm particles in Fig. 2 (white arrow 1) are PEG molecules. Carbon adsorbs very easily on copper electrodeposited surfaces exposed to air and diffusion pump oil in FE-Auger spectroscopy. These contaminations may result in the same amount of carbon peaks in points 1 and 2. Furthermore, in our previous paper,[8] the diameters of PEG particles of molecular weight 1000 are one-third the size formed by PEG of molecular weight 7500. Combustion analysis of the electrodeposit films detected ten times the carbon and three times the oxygen from an electrodeposited film with PEG and Cl^- additives compared to an electrodeposited film without PEG and Cl^- additives. Hence, we conclude that the several 10 nm particles observed by the FE-SEM are PEG molecules.

PEG molecules and QCM.—Initially pure copper was electrodeposited on the QCM substrates from a basic bath consisting of $CuSO_4$ and H_2SO_4 only. These substrates were immersed in the bath of $CuSO_4$ and H_2SO_4 with PEG and Cl^- additives. Figure 4 shows the frequency deviation-time curves measured by QCM. Figure 4a is the QCM curve when the substrate was immersed in the bath of $CuSO_4$ and H_2SO_4 without PEG and Cl^- additives. The frequency deviation is almost constant and does not increase with time. Figure 4b is the QCM curve when the substrate was immersed in a bath of $CuSO_4$ and H_2SO_4 with PEG and Cl^- additives. The frequency deviation increases markedly within 100 s and increases slightly after 500 s.

Figure 4c is a FE-SEM micrograph of copper electrodeposit immersed for 200 s into the bath of $CuSO_4$ and H_2SO_4 with PEG and Cl^- additives. The crystal surfaces are flat but several 10 nm PEG molecules exist. Figure 4d is that immersed for 1000 s. Crystal

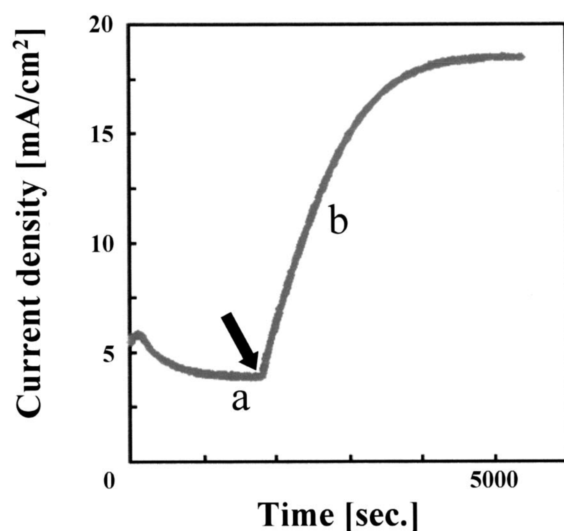

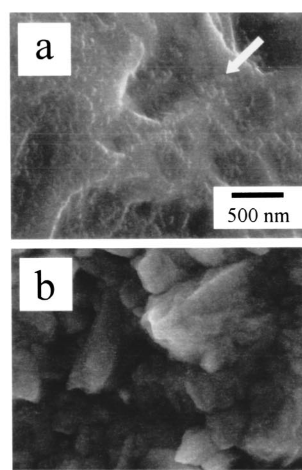

Figure 5. Current density-time curve, and FE-SEM micrographs of electrodeposits: (a) before adding SPS additive with 1800 s and (b) after adding SPS additive with 3000 s.

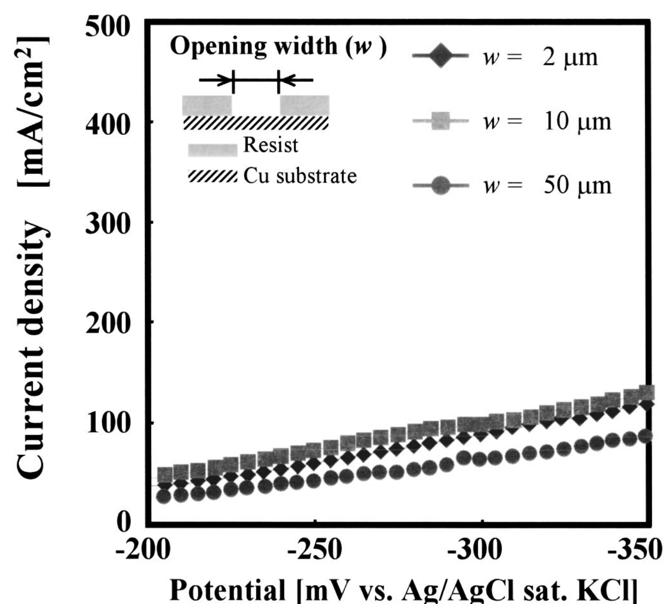

Figure 6. Current-density/potential curves for through-mask cathode at opening width, $w = 2$, 10, and 30 μm. Electrodeposition with additives of $Cl^- + PEG + JGB$. The inset shows the illustration of through-mask cathode used this voltammetry.

surfaces are also flat, but numerous several 10 nm PEG molecules exist. These FE-SEM micrographs of c and d correspond to the increase in QCM frequency deviation in b.

PEG molecules and SPS additives.—Figure 5 is the current density-time curve with the bath of $CuSO_4$ and H_2SO_4 with PEG and Cl^- additives. Initially, the current density shows a constant value at a lower current density of 4.3 mA/cm^2. After 1800 s, 1 ppm of SPS was added to the bath (indicated with an black arrow in Fig. 5, and the current density markedly increased with time. After 4000 s, the current density became constant with time and remained at 18.5 mA/cm^2. SPS additive has an acceleration effect, and increases the current density drastically.

Figure 5a is the FE-SEM micrograph of copper electrodeposited at 1800 s from the bath of $CuSO_4$ and H_2SO_4 with PEG and Cl^- additives. Numerous PEG molecules (indicated with white arrow) exist, and the crystal diameter is about 500 nm. After SPS is added at 3000 s (Fig. 5b), the PEG molecules are no longer present. The crystal diameters become 100 nm and refinement occurs. The SPS additive has the effect of removing PEG molecules from copper electrodeposited surfaces and of refining copper electrodeposited crystals.

Acceleration effect, electrochemical detection by through-mask cathode.—The through-mask cathode is known to detect the via bottom acceleration effect by SPS.[7-9] Through-mask cathodes consist of pattern widths of 2, 10, and 30 μm and are illustrated in the inset in Fig. 6. The current-density/potential curves without SPS were measured for different opening widths of through-mask cathodes. The additives were PEG, Cl^-, and JGB (Fig. 6). Without SPS, it is clear that the current density does not depend on the opening widths of through-mask cathodes.

Next, the current-density/potential curves with SPS were measured for different opening widths of through-mask cathodes. Figure 7 shows the current-density/potential curves with additives of (a) $Cl^- + PEG + SPS$ and (b) $Cl^- + PEG + SPS + JGB$. The opening widths are 2, 10, and 30 μm. It is clear that the current density depends on the opening widths. The narrower the opening widths, the greater the current densities. The through-mask cathodes detected the via bottom acceleration effect. Moreover, it is clear that

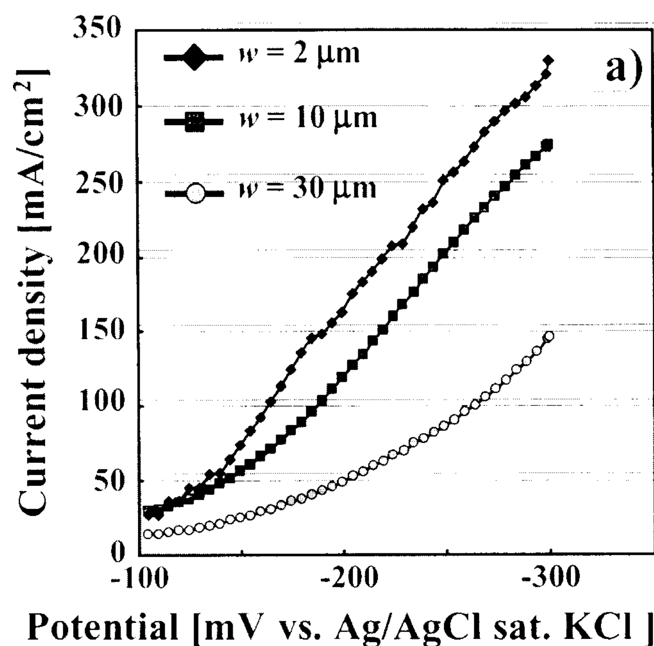

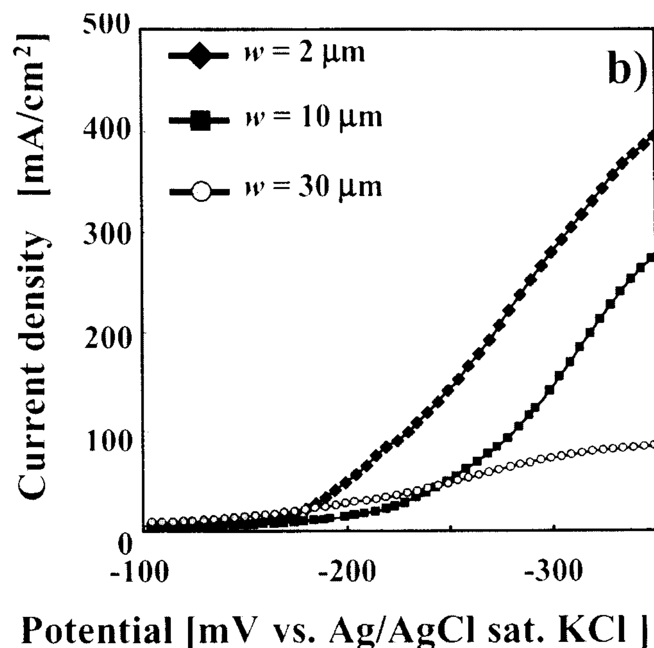

Figure 7. Current-density/potential curves for through-mask cathode at opening width, $w = 2$, 10, and 30 μm. Electrodeposition with additives of (a) $Cl^- + PEG + SPS$ and (b) $Cl^- + PEG + SPS + JGB$.

the via bottom current densities increase with decreasing width of the through-mask cathode and this occurs with (Fig. 7a) JGB and without (Fig. 7b) JGB. These current density increases are due to the via bottom acceleration effect of SPS.

From the view point of the detection of free cuprous and thiolate complex, we made a similar experiment to that done of Vereecken *et al.*[15] Figure 8 shows the results of our ring-disk electrode experiment in the case of 0.5 and 0.9 V of disk electrode. SPS oxidation occurs at potential of 0.9 V and no SPS oxidation occurs at 0.5 V.[15] Next, the ring electrode potential (E_{RING}) was fixed at 0.5 and 0.9 V. Since a larger I_{RING} was detected at SPS oxidation potential of 0.9 V, the hatched area in Fig. 8 must correspond to the oxidation of free SPS complex.

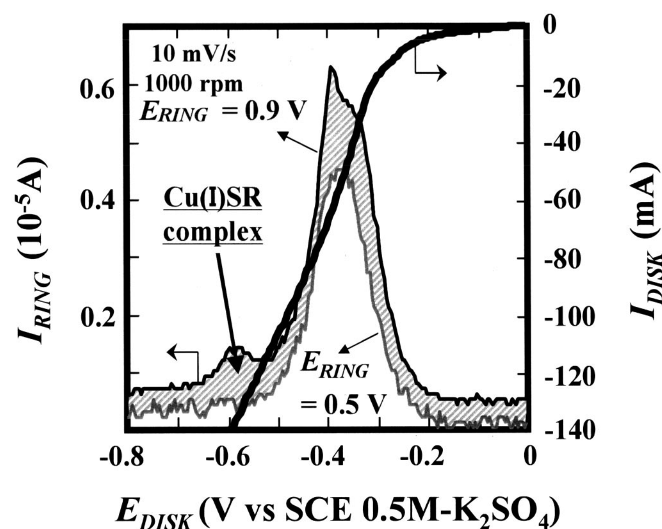

Figure 8. Rotating ring-disk voltammetry with additives of Cl^- + PEG + SPS.

Deposit cross sections on the through-mask cathodes.—Josell *et al.*[11] proposed an acceleration mathematical model based on the curvature formation at via bottom. Since narrower opening widths of through-mask cathodes (2 and 10 μm) show an acceleration effect (Fig. 7), the deposited cross sections on the through-mask cathodes were observed in order to identify the existence of the curvatures (Fig. 9). The additives are PEG + Cl^- + JGB + SPS. It was found that the deposits are always flat, and no curvature was observed. The deposit curvature is thus not the origin of the acceleration effect.

Figure 10 shows the schematic illustration of the inhibition and acceleration effects of the Damascene electrodeposition. PEG molecules inhibit the electrodeposition reaction by adsorption on the copper electrodeposit. The free acceleration complex of cuprous and thiolate forms. With narrower via opening width, the acceleration complex accumulates within the via. This increases the via bottom current density and accelerates the via bottom growth. This model is based on the free acceleration complex of cuprous and thiolate. The acceleration complex that accumulates within the vias may also remove the via bottom PEG molecules adsorption, as has been observed in Fig. 5b.

Conclusions

The role of additives for copper Damascene has been discussed experimentally based on electrodeposit morphology, FE-Auger, QCM, and electrochemical measurements with a through-mask cathode.

Particles several tens of nanometers in size were observed by FE-SEM on copper surfaces after an electrodeposition time of 60 min.

These particles show stronger FE-Auger spectrum oxygen-peak intensity than bare copper electrodeposit surfaces. PEG is an oxygen-containing polymer, and these particles observed by the secondary electron image of FE-SEM are PEG molecules.

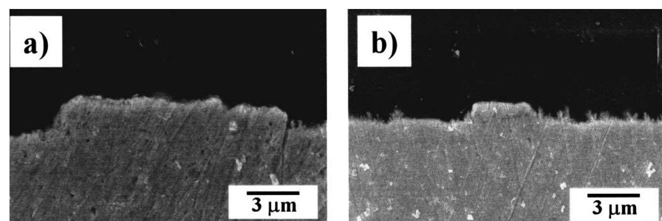

Figure 9. SEM micrographs of cross sections formed in the through-mask cathode at w = (a) 10 and (b) 2 μm. See Fig. 7b for the conditions of electrodeposition.

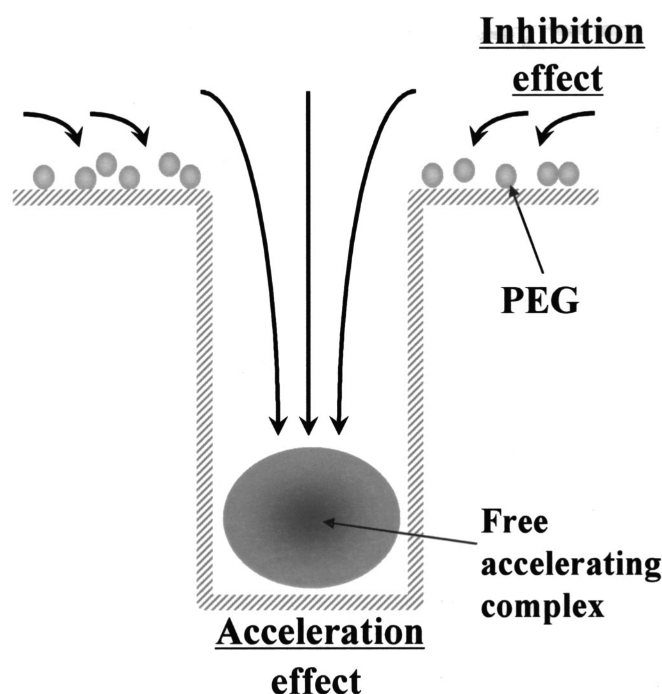

Figure 10. Schematic illustrations of inhibition and acceleration effects.

The QCM substrates were immersed into $CuSO_4$ and H_2SO_4 solution without PEG and Cl^- additives. The QCM frequency deviation does not increase with time. When the substrates were immersed into $CuSO_4$ and H_2SO_4 solution with PEG and Cl^- additives, the QCM frequency deviation markedly increase within 100 s. Numerous PEG molecules were observed by FE-SEM on the substrate.

The current density shows a constant, low value of 4.3 mA/cm^2 with the bath of $CuSO_4$ and H_2SO_4 with PEG and Cl^- additives. Once 1 ppm of SPS was added to the bath, the current density started to increase markedly with time. The SPS additive is an accelerator which increases the current density drastically. Numerous PEG molecules were present on the surface before the addition of SPS. No PEG molecules were present after SPS was added to the bath. Refinement of the copper electrodeposit occurs, and the crystal diameter shrinks to 100 nm. The SPS additive has the effect of removing PEG molecules and refines the deposit grain structure.

The PEG molecules were observed by the secondary electron image of FE-SEM and this observation was *ex situ*. During the electrodeposition process, more PEG molecules should adsorb on copper electrodeposited surface from their initial stage. This adsorption was monitored by QCM within the first 100 s (as indicated above). These PEG molecules should inhibit the electrodeposition during copper Damascene process.

The current density on the through-mask cathodes increased with narrower opening widths of the through-mask. Even though the current density markedly increased, the deposited cross sections on narrower opening widths of 2 and 10 μm were flat and no curvatures were found. The deposit curvature is not the origin of the acceleration effect.

Acknowledgments

We thank Dr. P. M. Vereecken at IBM T. J. Watson Research Center for instructive discussions. We also thanks Professor M. Seo of Hokkaido University for the rotating ring-disk electrode.

The Okayama University assisted in meeting the publication costs of this articles.

References

1. M. Yokoi, S. Konishi, and T. Hayashi, *Denki Kagaku oyobi Kogyo Butsuri Kagaku,* **52**, 218 (1984).
2. J. J. Kelly and A. C. West, *J. Electrochem. Soc.,* **145**, 3472 (1998).
3. J. J. Kelly and A. C. West, *J. Electrochem. Soc.,* **145**, 3477 (1998).
4. J. J. Kelly, C. Tian, and A. C. West, *J. Electrochem. Soc.,* **146**, 2540 (1999).
5. P. C. Andricacos, C. Uzoh, J. O. Dukovic, J. Horkans, and H. Deligianni, *IBM J. Res. Dev.,* **42**, 567 (1998).
6. K. Kondo, N. Yamakawa, Z. Tanaka, and K. Mano, *J. Jpn Inst. Electron. Packag.,* **4**, 1 (2001).
7. K. Kondo, N. Yamakawa, and K. Hayashi, Abstract 358, The Electrochemical Society Meeting Abstracts, Vol. 2000-1, Toronto, Ontario, Canada, Meeting, May 14-18, 2000.
8. K. Kondo, K. Hayashi, Z. Tanaka, and N. Yamakawa, *J. Jpn Inst. Electron. Packag.,* **3**, 607 (2000).
9. K. Kondo, N. Yamakawa, Z. Tanaka, and K. Hayashi, *J. Appl. Electrochem.,* in press.
10. J. Reid, S. Mayer, E. Broadbent, E. Klawnhn, and K. Ashtiani, *Solid State Technol.,* **2000**, 80.
11. D. Josell, D. Wheeler, W. H. Huber, J. E. Bonevich, and T. P. Moffat, *J. Electrochem. Soc.,* **148**, C767 (2001).
12. A. C. West, S. Mayer, and J. Reid, *Electrochem. Solid-State Lett.,* **4**, C50 (2001).
13. H. Deligianni, J. Horakans, K. Kwietniak, J. O. Dukovic, P. C. Andricacos, S. Boettcher, S.-C. Seo, P. Locke, A. Simon, S. Seymour, and S. Malhotra, Abstract 368, The Electrochemical Society Meeting Abstracts, Vol. 2000-1, Toronto, Ontario, Canada, May 14-18, 2000.
14. E. Farndon, F. C. Walsh, and S. A. Campbell, *J. Appl. Electrochem.,* **25**, 572 (1995).
15. P. Vereecken, H. Deligianni, K. T. Kwitniak, and P. C. Andricacos, Abstract 517, The Electrochemical Society Meeting Abstracts, Vol. 2002-1, Philadelphia, PA, May 12-17, 2002-1.